Miralem HADŽISELIMOVIĆ[1,2], Matic BLAZNIK[2], Bojan ŠTUMBERGER[1,2], Ivan ZAGRADIŠNIK[2]

University of Maribor, Faculty of Energy Technology (1)
University of Maribor, Faculty of Electrical Engineering and Computer Science (2)

Magnetically Nonlinear Dynamic Model of a Series Wound DC Motor

***Abstract**. This paper deals with mathematical modeling of a series wound DC motor, where magnetic nonlinearities play a big role. Three different models are presented: magnetically linear dynamic model and two different types of magnetically nonlinear dynamic models. Magnetically nonlinearities of iron core are taking into account with definitions of static and dynamic inductances. Each model has been evaluated on the basis of results obtained by simulations and results of measurements conducted on a tested motor.*

***Streszczenie.** W artykule przedstawiono metodykę modelowania matematycznego silników DC z szeregowym uzwojeniem, w którym nieliniowości magnetyczne grają dużą rolę. Zaprezentowano trzy modele: model z liniowością magnetyczną, dwa modele o różnej nieliniowości magnetycznej. Nieliniowość magnetyczna rdzenia jest rozpatrywana pod kątem statycznej i dynamicznej indukcyjności. Każdy model został ewaluowany na podstawie wyników otrzymanych w symulacji i w pomiarach testowego silnika. (**Magnetycznie nieliniowy dynamiczny model silnika DC z szeregowym uzwojeniem**)*

Keywords: series wound DC motor, modelling, magnetically nonlinearities, static and dynamic inductances
Słowa kluczowe: silnik DC szeregowy, modelowanie, nieliniowość magnetyczna, indukcyjności statyczne i dynamiczne

Introduction

Series wound motors (SWMs) are being used in drives where a big initial torque has to be provided (e.g. electric trains, trams, escalators, conveyor belts etc.). It could be also found in many milling machines, hand tools and household appliances, known as universal motor, supplied by either AC or DC current.

Often, it is not possible to do experimental analysis in reality, due to the dangerous circumstances or the drive system is simply out of range. For this reason mathematical models are used to perform safe analysis of dynamic and steady state operations. Moreover, mathematical models are convenient for control design purposes [1,2]. On the base of proposed magnetically nonlinear dynamic model, the control has been designed [3]. As a result, control was faster and less energy was used.

The main aim of the research is to provide a well working dynamic model of a SWM, considering magnetic nonlinearities. From a simple magnetically linear dynamic model, two different types of magnetically nonlinear dynamic models have been derived, taking into account characteristics of static and dynamic inductances [4]. Furthermore, experimental methods for determining parameters and characteristics of flux linkages are explained, which are needed for simulation calculations [5,6]. Based on results of aforementioned calculations and results obtained by measurements on the tested motor each of derived models has been evaluated.

Theoretical background of SWM operation

SWM is a type of DC electric motor with very uncommon torque and speed characteristics, due to the series connection of main and armature field windings [7].

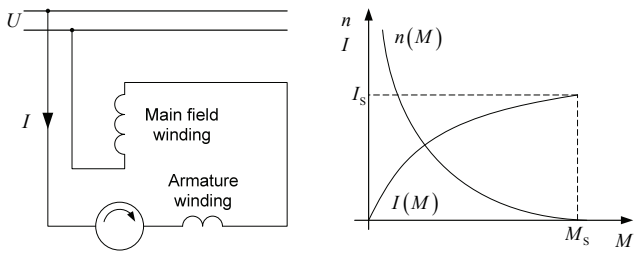

Fig.1. Windings connection and characteristics of a SWM

Low-resistance main field winding is located around outstanding poles on stator, meanwhile armature winding is located on rotor. Galvanic connection between armature winding and main winding is achieved by commutator which consists of brushes and commutator segments (Fig. 2). Current passes through the main winding, creating the main magnetic field. The same current also passes through the armature winding which is now exposed to main magnetic field. The result is a pair of forces, which cause a rotation. To achieve continuous torque, the appropriate coils of the armature winding have to be turned on in the exact moment of time, which is provided by commutator. Nominal values of tested SWM are presented in Table 1.

Table 1. Nominal values of sample SWM

Nr. of poles	2	-
Voltage	220	V
Current	9	A
Power	1,5	kW
RPM	1500	min^{-1}

Modeling of SWM

Magnetically nonlinear model of SWM has been derived on the basis of differential equations that describe the dynamics of motor's electrical and mechanical subsystems [8]. At first, linear model has been derived, taking into account electrical (1) and mechanical (2) equation, describing each subsystem:

$$u = \left(R_{\mathrm{m}} + R_{\mathrm{a}}\right) i + \left(L_{\mathrm{m}} + L_{\mathrm{a}}\right) \frac{\mathrm{d}i}{\mathrm{d}t} + L_{\mathrm{ma}}\, \omega\, i \tag{1}$$

where: u - terminal voltage, i - corresponding current, R - resistance of winding, L - linearized inductance and indexes m - main field, a - armature field.

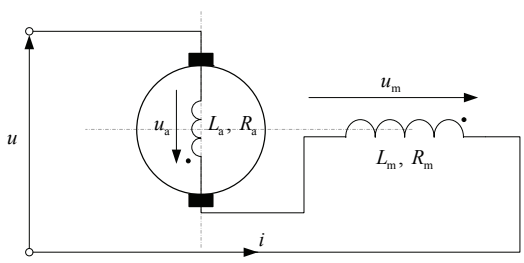

Fig.2. Electrical subsystem of SWM

Mechanical subsystem is being described by Newton's law of inertia for rotating object.

(2) $$J\frac{\mathrm{d}\omega}{\mathrm{d}t} = m_\mathrm{e} - m_\mathrm{l} - m_\mathrm{fr}$$

Where: J - rotor inertia, ω - angular speed, m_e, m_l, m_fr - electromagnetic, load and friction torque.
The relationship between both subsystems can be obtained through the balance of energy and mechanical power p:

(3) $$m_\mathrm{e} = \frac{p}{\omega} = i^2 L_\mathrm{ma}\,.$$

Considering all three equations, the magnetically linear dynamic model of SWM can be defined. Schematic presentation of magnetically linear dynamic model is presented in Fig. 3.

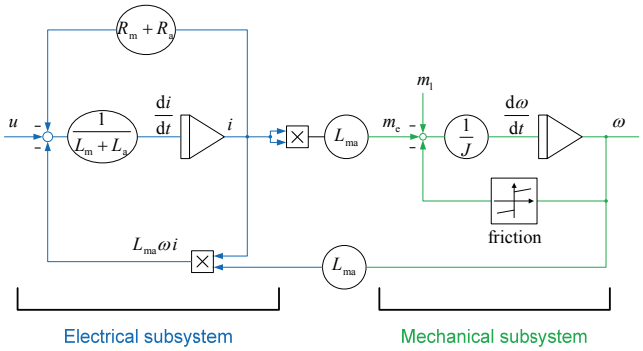

Fig.3. Block diagram of SWM magnetically linear dynamic model

For a magnetically linear dynamic model the inductances are constants and are determined with linearization in the operating point as a quotient of flux linkage Ψ and corresponding current i.

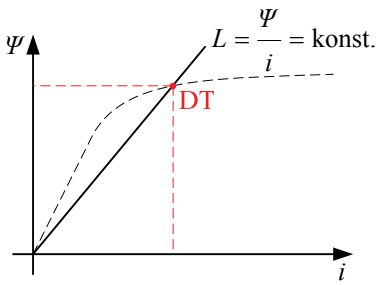

Fig.4. Determination of inductances for the magnetically linear model of SWM

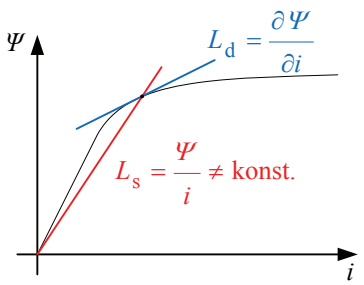

Fig.5. Determination of static and dynamic inductances

As is known, the magnetic material in stator in rotor is not as ideal as they are presented in magnetically linear models. In order to consider magnetic nonlinearities it is necessary to introduce the definition of static L_s and dynamic L_d inductances, which indirectly describing the characteristic of entire magnetic circuit [4]. To involve previously defined inductances in the model of SWM, the equation of electrical subsystem has to be modified, meanwhile the equation of mechanical subsystem stays unchanged. Additionally, the equation which is connecting both subsystems has to be changed in the same way. At first, the static inductance will be considered in the mentioned equations:

(4) $$u = \left(R_\mathrm{m}+R_\mathrm{a}\right)i + \left(\frac{\Psi_\mathrm{m}(i)}{i}+\frac{\Psi_\mathrm{a}(i)}{i}\right)\frac{\mathrm{d}i}{\mathrm{d}t} + \Psi_\mathrm{ma}(i)\,\omega\,,$$

(5) $$m_\mathrm{e} = \frac{p}{\omega} = i\,\Psi_\mathrm{ma}(i)\,.$$

Regarding to (4) and (5) the magnetically nonlinear dynamic model of SWM can be expressed. Magnetically nonlinear magnetic model using static inductances L_s is presented in Fig. 6.

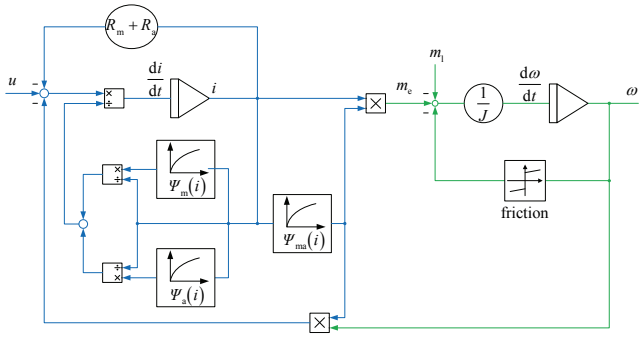

Fig.6. Block diagram of SWM magnetically nonlinear dynamic model using static inductances L_s

As well as definition of static inductance L_s, the dynamic inductance L_d can be used in the model of SWM. Dynamic inductances are written in form of flux linkage partial derivatives and can be used in (4) and (5). Consequently voltage balance and torque equations can be written for SWM magnetically nonlinear dynamic model using dynamic inductances:.

(6) $$u = \left(R_\mathrm{m}+R_\mathrm{a}\right)i + \left(\frac{\partial\Psi_\mathrm{m}}{\partial i}+\frac{\partial\Psi_\mathrm{a}}{\partial i}\right)\frac{\mathrm{d}i}{\mathrm{d}t} + \frac{\partial\Psi_\mathrm{ma}}{\partial i}\,\omega i\,,$$

(7) $$m_\mathrm{e} = \frac{p}{\omega} = i^2\,\frac{\partial\Psi_\mathrm{ma}}{\partial i}\,.$$

Corresponding schematic presentation of magnetically nonlinear model using dynamic inductances is presented in Fig. 7.

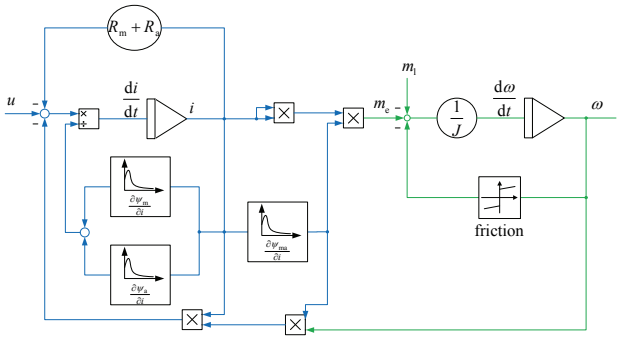

Fig.7. Block diagram of SWM magnetically nonlinear dynamic model using dynamic inductances L_d

Experimental determination of flux linkages characteristics and parameters of electrical subsystem

To provide reliable simulations [9], parameters and characteristics should be measured accurately as much as possible. For this reason, the experimental setup has been established, which is schematically shown in Fig. 8. Various types of sources have been used to provide either AC or DC voltage. As a load 4Q close-loop controlled AC drive has been used and was coupled to the test motor through the torque sensor and clutches. All values have been measured by power analyzer and further analysed by computer using numerical methods.

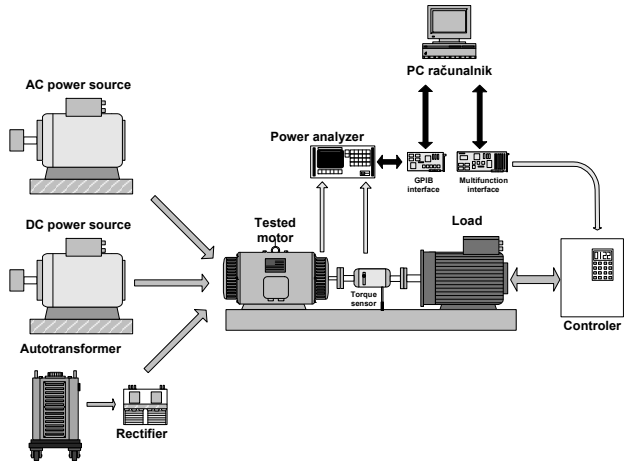

Fig.8. Established experimental setup

First set of tests contains determination of electrical subsystem's parameters and flux linkages. The resistance of each winding has been measured by four wire voltage-current method. The rotor has been locked during the test.

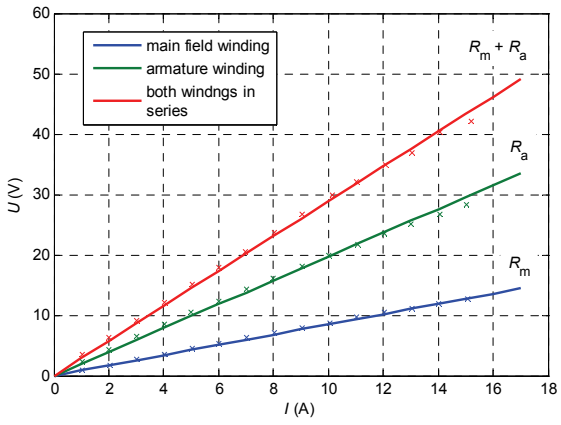

Fig.9. Results of resistance measurements

Next, characteristics of flux linkages have been determined including self flux linkage of main winding Ψ_m, self flux linkage of armature winding and mutual flux linkage Ψ_{ma}. Self flux linkages have been determined separately by supplying each winding with AC voltage and with measuring time waveforms of voltage and current. Considering measured time waveforms the characteristics of self flux linkages have been determined by numerical integration of induced voltage:

$$\Psi(t) = \int_0^t \left[u(\tau) - Ri(\tau)\right] \mathrm{d}\tau + \Psi(0). \tag{8}$$

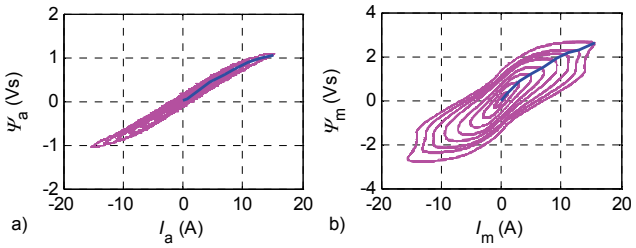

Fig.10. Characteristics of self flux linkages: a) armature winding and b) main field winding

In case of non-laminated iron core, measurements should be obtained at the lowest possible frequency, which could be provided by experimental setup. Otherwise, the eddy currents effect would rapidly influence the characteristics of flux linkages.

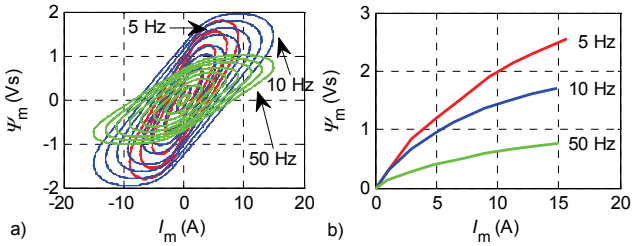

Fig.11. Influence of eddy currents effect on characteristics of flux linkages (green – 50 Hz, blue – 10 Hz and red 5 Hz)

The characteristics of static and dynamic inductances have been calculated from characteristics of flux linkages, using numerical methods.

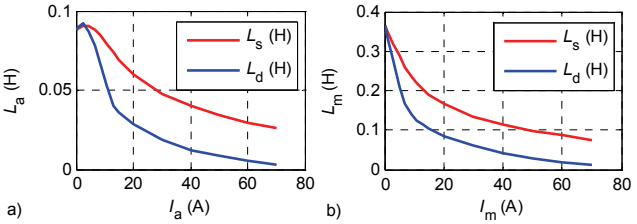

Fig.12. Characteristics of self static and dynamic inductances: a) armature winding and b) main field winding

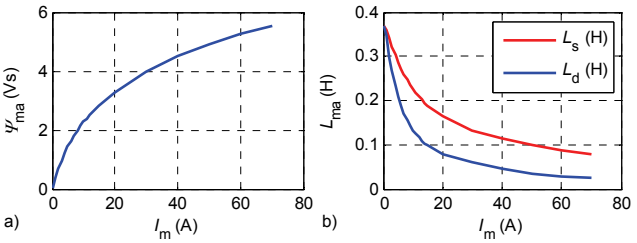

Fig.13. Characteristics of: a) mutual flux linkage and b) mutual static and dynamic inductances

Moreover, determination of the characteristic of mutual dynamic and static inductance has been done on the basis of mutual flux linkage measurement. Meanwhile the motor shaft has been constantly turning by the speed controlled AC drive, the main field winding has been powered by DC voltage. Considering measured values of main field winding current I_m and induced voltage E_a in armature winding, the characteristic of mutual dynamic inductance L_{mad} can be determined:

$$L_{mad} = \frac{E_a}{\omega I_m}. \tag{9}$$

As a result, characteristic of mutual flux linkage and static inductance can be calculated on the basis of (10):

$$\Psi(i) = \int_0^i L_{\mathrm{d}}\,\mathrm{d}i \,. \tag{10}$$

At this point, it is important to mention that all characteristics of flux linkages and inductances have been extrapolated for the needs of simulations. In addition, linearization of the above characteristics is necessary to perform simulations of the linear model. The linearization has been carried out at the operating point defined by nominal values (Table 1).

Experimental determination of friction torque characteristics and parameters of mechanical subsystem

Second set of tests includes determination of the mechanical subsystem's parameters which are characteristics of friction torque and rotor inertia. It is important to take into account friction and inertia of whole drive system to assure relevant and accurate simulations. For this reason the characteristic of friction has been measured for both, tested motor and load motor. In general, it is composed of Coulomb and viscous friction, also presented in Fig.14. According to those measurements and (11), the drive shaft inertia has been determined on the basis of the run-out measurement.

$$J\frac{\mathrm{d}\omega}{\mathrm{d}t} = m_{\mathrm{fr}} \tag{11}$$

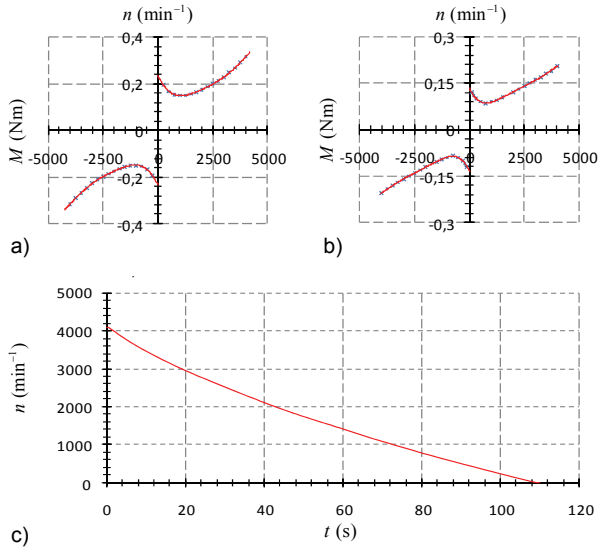

Fig.14. Friction characteristics of: a) tested motor, b) load motor and c) run-out measurement

Comparison of measured and simulated responses

Calculated responses for all three presented models (linear model, magnetically nonlinear dynamic model using static inductances and magnetically nonlinear dynamic model using dynamic inductances) have been executed in software package Matlab/Simulink. Characteristics of static and dynamic inductances have been considered as the tabulated list of values in the form of look-up table block. Time responses have been calculated using Runge-Kutta method for numerical integration. Scenarios like start with additional inertia and locked-rotor start have been performed on the tested motor. To assure reliable results, the actual supplied voltage had been measured and considered in simulations.

Locked-rotor response test has been performed at lowered voltage otherwise high current could damage windings. During this type of test the mechanical subsystem is not active, because rotation is not present. For this reason, locked-rotor test presents how accurately the parameters of electrical subsystem and flux linkage characteristics have been determined. Measured and calculated values of time responses are presented in Fig.15.

Considering torque and speed characteristics, it is impossible to perform free-run response test [10], because endless rising of speed would destroy tested motor. Therefore, the inertia and friction of load motor have been used to prevent uncontrolled behaviour of tested motor. Measured and calculated values of time responses are presented in Fig.16.

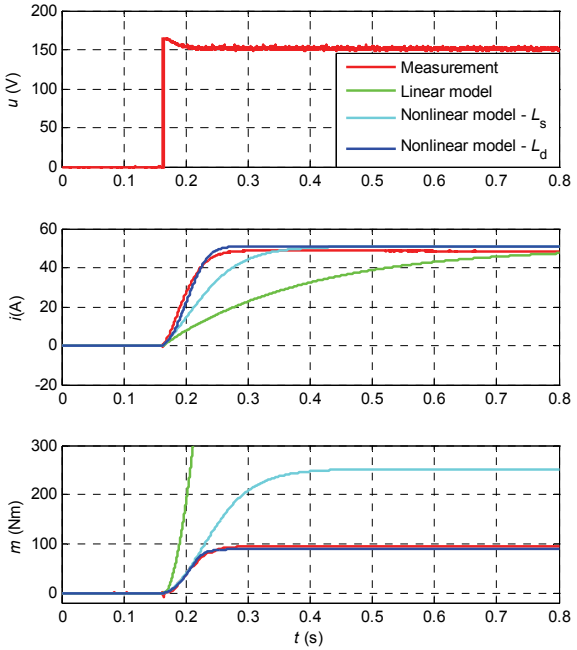

Fig.15. Comparison of simulation results and measurements of locked-rotor response test, $U = 150$ V

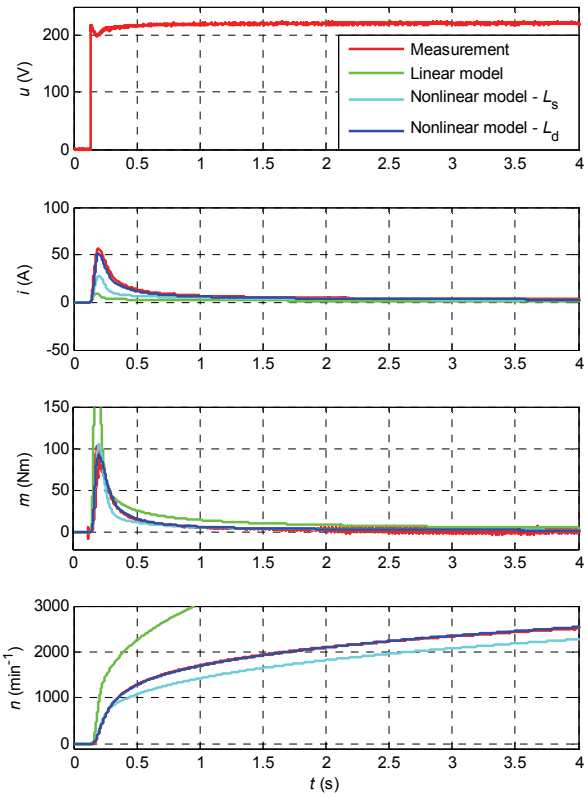

Fig.16. Comparison of simulation results and measurements of response test with additional load, $U = 220$ V

Conclusion

Comparison of measured and calculated time responses shows, that magnetically linear model is highly inaccurate and it is only useful for steady state operation analysis. Both magnetically nonlinear dynamic models have provided better results. Dynamic model considering characteristics of static inductances has resulted quite accurate time responses. This type of model is useful only when analysis of crossing from one to another steady state operation is needed, hence no dynamic accuracy is necessary. Magnetically nonlinear dynamic model using dynamic inductances has provided the most accurate calculated results, therefore it can be used not only for steady state analysis, but also for dynamic operation analysis. Aforementioned model is very useful for control design purposes.

Finally, the best resulting magnetically nonlinear dynamic model of a series wound DC motor has been derived and could be also used for simulation calculations of AC SWMs (e.g. universal motors). Moreover, this research offers further possibilities to improve calculated time responses. For example magnetic nonlinearities and iron losses could be included in the modeling procedure by using Jill-Atherton's model.

REFERENCES

[1] A. Chowdhury, A. Sarjaš, P. Cafuta, R. Svečko, Robust controller synthesis with consideration of performance criteria, *Optim. control appl. methods*, December 2010.

[2] A. Sarjaš, R. Svečko, A. Chowdhury, Strong stabilization servo controller with optimization of performance criteria, *ISA Transactions*, 2011, vol. 50, 419-431.

[3] D. Igrec, A. Sarjaš, A. Chowdhury, QFT-based robust velocity controller design for a SW-DC motor, *Przegląd Elektrotechniczny*, 2011, vol. 87, No. 3, 81-84.

[4] Štumberger G., Plantić Ž., Štumberger B., Marčič T., Impact of static and dynamic inductance on calculated time response. *Przegląd Elektrotechniczny*, 2011, vol. 87, No. 3, 190-193.

[5] M. Kuczmann, Vector Preisach Hysteresis Modeling: Measurement, Identification and Application, *Physica B*, 2011, Vol. 406, pp. 1403-1409.

[6] M. Kuczmann, A. Iványi, The Finite Element Method in Magnetics, *Akadémiai Kiadó (Academic Press)*, Budapest, 2008.

[7] I. Zagradišnik, B. Slemnik, Rotating electrical machines, *University of Maribor (Academic Press)*, Maribor, 2009.

[8] D. Dolinar, G. Štumberger, Modeling and control of electromechanical systems, *University of Maribor (Academic Press)*, Maribor, 2006.

[9] T. Marčič, A short review of energy-efficient line-start motor design. *Przegląd Elektrotechniczny*, 2011, vol. 87, No. 3, 119-122.

[10] T. Marčič, Experimental evaluation of the impact of squirrel-cage material on the performance of induction motors and line-start interior permanent magnet synchronous motors. *Przegląd Elektrotechniczny*, 2011, vol. 87, No. 9a, 334-337.

***Authors**: Miralem Hadžiselimović, Bojan Štumberger University of Maribor, Faculty of Energy Technology, Hočevarjev trg 1, 8270 Krško, Slovenia, E-mail: miralem.h@uni-mb.si; Matic Blaznik, Ivan Zagradišnik University of Maribor, Faculty of Electrical Engineering and Computer Science, Smetanova 17, 2000 Maribor, Slovenia.*